Biogeosciences Discuss., 11, 8085–8113, 2014
www.biogeosciences-discuss.net/11/8085/2014/
doi:10.5194/bgd-11-8085-2014

Biogeosciences Discussions
Open Access

Components of near-surface energy balance derived from satellite soundings – Part 2: Latent heat flux

K. Mallick[1], A. Jarvis[2], G. Wohlfahrt[3], G. Kiely[4], T. Hirano[5], A. Miyata[6], S. Yamamoto[7], and L. Hoffmann[1]

[1]Department of Environment and Agro-biotechnologies, Centre de Recherche Public – Gabriel Lippmann, L4422, Luxembourg
[2]Lancaster Environment Centre, Lancaster University, LA1 4YQ, UK
[3]Ecosystem Research & Landscape Ecology, University of Innsbruck, 6020 Innsbruck, Austria
[4]Hydrometeorology Research Group, Department of Civil and Environmental Engineering, University College Cork, Ireland
[5]Division of Environmental Resources, Research Faculty of Agriculture, Hokkaido University, Hokkaido, Japan
[6]National Institute for Agro-Environmental Sciences, Tsukuba, Japan
[7]Graduate School of Environmental Science, Okayama University Tsushimanaka 3-1-1, Okayama 700-8530, Japan

Received: 27 March 2014 – Accepted: 21 May 2014 – Published: 4 June 2014

Correspondence to: K. Mallick (mallick@lippmann.lu)

Published by Copernicus Publications on behalf of the European Geosciences Union.

BGD
11, 8085–8113, 2014

Abstract

This paper introduces a relatively simple method for recovering global fields of latent heat flux. The method focuses on specifying Bowen ratio estimates through exploiting air temperature and vapour pressure measurements obtained from infra-red soundings of the AIRS (Atmospheric Infrared Sounder) sensor onboard the NASA-Aqua platform. Through combining these Bowen ratio retrievals with satellite surface net available energy data we have specified estimates of global surface latent heat flux at the 1° by 1° scale. These estimates were evaluated against data from 30 terrestrial tower flux sites covering a broad spectrum of biomes. Taking monthly average 13:30 h data for 2003, this revealed a relatively good agreement between the satellite and tower measurements of latent heat flux, with a pooled root mean square deviation of 79 W m^{-2}, and no significant bias. However, this success partly arose as a product of the under specification of the AIRS Bowen ratio compensating for the under specification of the AIRS net available energy.

1 Introduction

The specter of increasing global surface temperatures mean our ability to both monitor and predict changes in the activity of the water cycle becomes critical if we are to develop the adaptive capability needed to manage this change (Lawford et al., 2004). As a result, significant investments have been and are being made in developing both monitoring and modelling capacity in the related areas of water resource management (Nickel et al., 2005), flood and drought risk assessment (Lehner et al., 2006) and weather and climate prediction (Irannejad et al., 2003; Brennan and Lackmann, 2005). Of the various components of the water cycle, the accuracy with which evaporative fluxes, E (or latent heat fluxes, λE), are both measured and hence modelled at scales relevant to decision making has been identified as an area where greater capacity is

BGD
11, 8085–8113, 2014

needed, particularly in order to evaluate and hence better constrain model performance (Chen and Dudhia, 2001; McCabe et al., 2008).

Satellites offer a potentially attractive source of data for calculating E at scales directly relevant to model development (Jiminez et al., 2009). Over the past 30 years a variety of schemes for specifying E using remote sensing data have been developed and used to evaluate the spatio-temporal behaviour of evaporation for field (Tasumi et al., 2005), regional (Bastiaanssen et al., 1998; Mu et al., 2007; Mallick et al., 2007) and continental scales (Anderson et al., 2007). The methods employed thus far appear to fall into several categories. The most common approach centres on assuming a physical model of evaporation given many of the terms required for these models are available as satellite products (Choudhury and Di Girolamo, 1998; Mu et al., 2007). A number of studies have also tried to resolve E indirectly by estimating the evaporative fraction from the relationship between satellite derived albedo, vegetation indices, and land surface temperature (Verstraeten et al., 2005; Batra et al., 2006; Mallick et al., 2009).

What is common to all these approaches is that they rely to a greater or lesser extent on parameterization of surface characteristics in order to derive the estimates of E and, therefore, the products from these approaches are conditional on these parameterizations. For example, in schemes which exploit the Penman–Monteith equation both the aerodynamic and surface resistance terms require some form of calibration of surface characteristics, often involving vegetation indices, whether empirically (Mu et al., 2007) or through linking to photosynthesis (Anderson et al., 2008). This is obviously a confounding factor when one attempts to use these data to evaluate surface parameterisations in weather, climate and hydrological models, particularly when the models we wish to evaluate may contain very similar model descriptions for E. What is required therefore are methods for deriving E estimates from satellite data that do not rely unduly on surface parameterisation so that they become a valid and valuable data source for model evaluation. One approach that appears to fulfill this requirement is where λE is estimated from satellite data as a residual term in the energy balance

BGD
11, 8085–8113, 2014

equation (Tasumi et al., 2005; Mallick et al., 2007). However, this approach suffers from the effects of error propagation because all errors including any lack of observed closure of the regional energy budget are lumped into the estimate of λE (Foken et al., 2006). From this we can see that something more akin to a satellite "observation" would be attractive.

Global polar orbiting sounders like AIRS (Atmospheric Infrared Sounder) provide profiles of air temperature and relative humidity at different pressure levels from the surface to the upper troposphere, along with several other geophysical variables (for example surface temperature, near surface air temperature, precipitable water, cloudiness, surface emissivity, geopotential height etc.). Profile information like this points to the possibility of exploiting Bowen ratio methods to produce large scale estimates of E. Despite having been used to refine estimate of near surface air temperature over the oceans (e.g. Hsu, 1998), the use of Bowen ratio methods in conjunction with satellite sounder data somewhat surprisingly appears to have been overlooked as a method for estimating E. The reasons for this are probably be twofold. Firstly, the resolutions of the temperature and humidity retrievals are assumed to be inadequate for differential methods like this. Secondly, there can be reservations over the applicability of the underlying assumptions of this method on this scale. Although these appear valid concerns there are important counter arguments to consider. Firstly, the degree of signal integration going on at the scale of the satellite sounding should help relax the requirement on signal resolution. This will be aided by an effectively large sensor separation in the vertical. Secondly, studies over both ocean and land indicate that the Bowen ratio method can be relatively robust under non-ideal conditions (Tanner, 1961; Todd et al., 2000; Konda, 2004). Given the potential benefits of having non-parametric estimates of E at the scales and spatial coverage offered by satellites, we argue that the possibility of using sounder products within a Bowen ratio framework merits investigation.

This paper presents a preliminary development and evaluation of 1° by 1° AIRS sounder-Bowen ratio derived latent heat flux, λE. We focus on terrestrial systems because of the availability of an extensive tower-based flux measurement network against

BGD
11, 8085–8113, 2014

which we can evaluate the various satellite derived components. However, we see no reason to exclude the oceanic estimates and refer to these where relevant.

2 Methodology

2.1 Bowen ratio methodology

The Bowen ratio (β) is the ratio of sensible, H ($\mathrm{W\,m^{-2}}$), to latent, λE ($\mathrm{W\,m^{-2}}$), heat flux (Bowen, 1926),

$$\beta = \frac{H}{\lambda E} \tag{1}$$

where λ is the latent heat of vaporization of water ($\mathrm{J\,kg^{-1}}$) and surface to atmosphere fluxes are positive. If the instantaneous energy balance of the plain across which H and λE are being considered is given by

$$\Phi = R_{\mathrm{N}} - G = \lambda E + H \tag{2}$$

where Φ ($\mathrm{W\,m^{-2}}$) is known as the net available energy, R_{N} ($\mathrm{W\,m^{-2}}$) is the net radiation across that plain and G ($\mathrm{W\,m^{-2}}$) is the rate of system heat accumulation below that plain, then combining Eqs. (1) and (2) one gets,

$$\lambda E = \frac{\Phi}{1+\beta} \tag{3}$$

Therefore, if Φ and β are available, λE can be computed (Dyer, 1974). The estimation of Φ from satellite data is covered in a companion paper (Mallick et al., 2014). β was estimated as follows.

H and λE are assumed to be linearly related to the vertical gradients in air temperature and vapour partial pressure, $\partial T/\partial z$ and $\partial p/\partial z$,

$$\lambda E = \rho \lambda \varepsilon k_{\mathrm{E}} \frac{\partial p}{\partial z} \tag{4a}$$

BGD
11, 8085–8113, 2014

and,

$$H = \rho c_p k_H \frac{\partial T}{\partial z} \tag{4b}$$

where ε is the ratio of the molecular weight of water vapour to that of dry air, ρ is air density ($\mathrm{kg\,m^{-3}}$), c_p is air specific heat ($\mathrm{J\,kg^{-1}\,K^{-1}}$), k_E and k_H are the effective transfer coefficients for water vapour and heat respectively ($\mathrm{m\,s^{-1}}$) (Fritschen and Fritschen, 2005). If heat and water vapour occupy the same transfer pathway and mechanism through a plain then $k_E \approx k_H$ (Verma et al., 1978) and Eqs. (1) and (4) reduce to,

$$\beta = \frac{c_p}{\lambda\varepsilon}\frac{\partial T}{\partial p} \tag{5}$$

suggesting β can be estimated from the relative vertical gradient in T and p (Bowen, 1926).

AIRS soundings for T and p are available for a range of pressure levels in the atmosphere (Tobin et al., 2006). Assuming the lowest available two pressure levels $p_{1,2}$ occur within a region of the planetary boundary layer within which Eqs. (4a) and (4b) hold, then a finite difference approximation of Eq. (5) gives,

$$\beta = \frac{c_p}{\lambda\varepsilon}\frac{(T_1 - T_2 + \Gamma)}{(p_1 - p_2)} \tag{6}$$

where Γ accounts for the adiabatic lapse rate in T which in this case will be significant. Here, the 1000 and 925 mbar pressure levels soundings will be exploited so that we are considering fluxes within the lower 1000 m of the atmosphere. For example, considering a landscape at zero meters above sea level, the 1000 mbar level would correspond to approximately 100 m and the 925 mbar level to 750 m, thus $\Delta z = 650$ m and the effective measurement height is, therefore, at approximately 400 m.

In the turbulent region of the atmosphere, eddy diffusivities for all the conserved scalars are generally assumed equal because they are carried by the same eddies

BGD
11, 8085–8113, 2014

and, therefore, are associated at source (Swinbank and Dyer, 1967). There is evidence to suggest k_H is greater than k_E under stable (early morning and late afternoon) conditions and when the effects of lateral advection of heat are significant (Verma et al., 1978). However, in the present study we use the 13.30 LT AIRS soundings to obtain T and p when the atmosphere will tend to be least stable and the average depth of the turbulent boundary layer should extend well beyond the 925 mbar level (Fisch et al., 2004). Also, we have opted to use the AIRS sounding data rather than its higher resolution MODIS counterpart because we anticipate lateral advection should be less of an issue at the larger scale.

The reliability of the estimates of β also depends on the accuracy and resolution of the measurements of the temperature and humidity gradients. The AIRS products are quoted as having resolutions and accuracies of $\pm 1\,\mathrm{K\,km^{-1}}$ for T and $\pm 10\,\%\,\mathrm{km^{-1}}$ for p (Aumann et al., 2003; Tobin et al., 2006). Given Bowen ratio studies are invariably applied to small sensor separations of the order of meters and at the point scale, precisions of $\pm 0.01\,^{\circ}\mathrm{C}$ for temperature and ± 0.01 kPa for vapour pressure are required (Campbell Scientific, 2005), making the AIRS sensitivities appear untenable. However, as mentioned above, the effective sensor separation of the order of hundreds of meters allied to the sounding integrating at the $10\,000\,\mathrm{km^2}$ scale should help lift these restrictions. Here we specify Γ following Eq. (6.15) in Salby (1996) which when rearranged gives:

$$\Gamma = \frac{\ln(T_2/T_1)\Gamma_d}{\ln(p_2/p_1)\kappa} \tag{7}$$

where Γ_d is the dry adiabatic lapse rate ($\sim 9.8\,\mathrm{K\,km^{-1}}$) and κ is the ratio of the specific gas constant ($\mathrm{J\,kg^{-1}\,K^{-1}}$) to the isobaric specific heat capacity ($\mathrm{J\,kg^{-1}\,K^{-1}}$) (Salby, 1996).

A general sensitivity/uncertainty analysis was carried out to assess the propagation of uncertainty through the calculation scheme onto the estimates of λE (see Mallick et al., 2014 for details).

BGD
11, 8085–8113, 2014

2.2 Satellite data sources

The AIRS sounder is carried by the NASA Aqua satellite, which was launched into a sun-synchronous low Earth orbit on 4 May 2002 as part of the NASA Earth Observing System (Tobin et al., 2006). It gives global, twice daily coverage at 1.30 a.m.–p.m. from an altitude of 705 km. In the present study we have used AIRS level 3 standard monthly products from 2003, with a spatial resolution of 1° by 1°. The monthly products are simply the arithmetic mean, weighted by counts, of the daily data of each grid box. The monthly merged product have been used here because the infrared retrievals are not cloud proof and the monthly products gave decent spatial cover in light of missing cloudy sky data. The data products were obtained in hierarchical data format (HDF4) with associated latitude-longitude projection from the NASA Mirador data holdings (http://mirador.gsfc.nasa.gov/). These datasets included all the meteorological variables required to realise Eqs. (6) and (7).

2.3 Tower evaluation data

The satellite estimates of β, λE, and H were evaluated against 2003 data from 30 terrestrial FLUXNET eddy covariance towers (Baldocchi et al., 2001) covering 7 different biome classes. These tower sites were selected to cover a range of hydrometeorological environments in South America, North America, Europe, Asia, Oceania and Africa. A comprehensive list of the site characteristics and the site locations are given in a companion paper Mallick et al. (2014) which describes the specification of the satellite net available energy used here.

Eddy covariance has largely replaced gradient-based methods like Bowen ratio as the preferred method for tower measurements of terrestrial water vapour and sensible heat flux. Because eddy covariance is not a gradient method it is an attractive source of evaluation data. Sensible and latent heat flux measurements were used as reported in the FLUXNET data base, in other words no corrections for any lack in energy balance closure (Foken, 2008; Wohlfahrt et al., 2009) were applied. The spatial scale of tower

BGD
11, 8085–8113, 2014

eddy covariance footprint is of the order of $< 10\,km^2$ and hence are at least three orders of magnitude smaller scale than the $10\,000\,km^2$ satellite data, which obviously has implications in heterogeneous environments.

3 Results

3.1 Bowen ratio – evaporative fraction evaluation

Figure 1a shows the global distribution of annual average, 13:30 LT β for 2003. The missing data segments are due to two data rejection criteria. Firstly, there are missing data in the AIRS sounder profiles, which are particularly prominent at high latitudes where presumably it is difficult to profile the atmosphere reliably near the surface and over the mountain belts where the lower pressure levels are intercepted by the ground. Secondly, we have imposed our own data rejection for β when there is reversal of the vertical vapour pressure gradient under high radiative load. This condition is often encountered in hot, arid settings when large scale advection causes the assumptions behind Bowen ratio methodology to become invalid (Rider and Philip, 1960; Perez et al., 1999). This condition was particularly prevalent over Australia in summer 2003 (Feng et al., 2008) and hence this region is not covered particularly well.

The first thing to note from Fig. 1a is that there is a clear land–sea contrast with β being relatively low and uniform over the sea as expected. The values of β over the oceans are in the region of 0.1, in line with commonly quoted figures for the sea (Betts and Ridgway, 1989; Hoen et al., 2002). Over the tropical forest regions of Amazonia and the Congo β is in the range 0.1 to 0.3, which also compares with values reported for these areas (da Rocha et al., 2004, 2009; Russel et al., 2006). The more arid areas are also clearly delineated. Although somewhat variable, the Sahara gives a range of 1.5–3.5 which corresponds with the results of Kohler et al. (2010) and Wohlfahrt et al. (2009) for the Mojave Desert. The South American savanna gives a range between 0.5–1 which corresponds with values reported by Giambelluca et al. (2009). One

BGD
11, 8085–8113, 2014

notable feature is the homogeneity of the β fields over the Americas in contrast to the heterogeneity over Eurasia. 2003 was associated with widespread drying over Europe (Fink et al., 2004) which may explain this feature.

Figure 2a shows the relationship between the satellite and tower derived estimates of evaporative fraction $\Lambda = (1+\beta)^{-1}$ (Shuttleworth et al., 1989). We have elected to evaluate β in terms of Λ because, unlike β, Λ is bounded and more linearly related to the tower fluxes from which it is derived ($\lambda E = \Lambda\Phi$, cf. Eq. 3). The evaluation in Fig. 2a reveals a significant correlation ($r = 0.34 \pm 0.06$[1]) between Λ (satellite) and Λ (tower), albeit one corrupted by significant variability. This is to be expected given β is defined as a ratio of either four uncertain soundings (for the satellite) or two uncertain fluxes (for the tower). Assuming both measures are co-related through some "true" intermediate scale variable then the relationship between the two for the data in Fig. 2a is given by Λ (satellite) = $0.31(\pm 0.02)\Lambda$ (tower) + $0.49(\pm 0.04)$ i.e. significantly different to 1 : 1.

The sensitivity analysis results are given in Table 1 and show a differentially higher sensitivity to the vapour pressure observations than for temperature, and a standard deviation of 0.11 on the estimates of Λ (satellite), although these results are dependent on the level of the input data given the inverse nonlinearity in Eq. (6).

3.2 Latent and sensible heat evaluation

Figures 1b and 2b show the geographical distribution of the average noontime net available energy and its evaluation for 2003 taken from Mallick et al. (2014). The corresponding geographical distributions of λE and H are shown in Fig. 1c and d. Figure 2c shows the relationship between the satellite and tower λE for all 30 evaluation sites. This gives an overall correlation of $r = 0.75(\pm 0.04)$. Assuming both the tower and satellite data are linearly co-related, linear regression gave λE (satellite) = $0.98(\pm 0.02)\lambda E$ (tower) (offset not significant) with a root mean square deviation (RMSD) of 79 W m^{-2} (see Fig. 2c). The biome specific statistics for λE are

[1] All uncertainties are expressed as ± one standard deviation unless otherwise stated.

BGD
11, 8085–8113, 2014

given in Table 2 which reveals correlations ranging between $r = 0.41(\pm 0.22)$ (SAV) to $r = 0.76(\pm 0.10)$ (ENF), RMSD ranging between 61 (MF) to 141 (SAV) W m^{-2} and regression gains ranging between 0.85(±0.08) (CRO) to 2.00(±0.28) (SAV).

The relationship between the satellite and tower H for all 30 evaluation sites is shown in Fig. 2d. Here, $r = 0.56(\pm 0.05)$ and H (satellite) = $0.59(\pm 0.02)H$ (tower) with an RMSD of 77 W m^{-2} for the pooled data. Again, the biome specific statistics for H are given in Table 2 and reveal correlations ranging between 0.43(±0.15) (GRA) to 0.79(±0.11) (CRO), RMSD ranging between 52 (CRO) to 149 (SAV) W m^{-2} and regression gains ranging between 0.45(±0.05) (SAV) to 0.93(±0.06) (CRO). Figure 3 shows some examples of monthly time series of λE for both the satellite and the towers for a range of sites. This reveals that the seasonality in λE (tower) is relatively well captured in λE (satellite) in the majority of cases with the exception of Vielsalm, Tsukuba and Skukuza. Therefore, the individual site statistics given in Table 2 largely reflect the seasonality in the tower data. Time series of the monthly full global fields of Φ and λE are available on http://www.lancs.ac.uk/staff/bsaajj.

The sensitivity–uncertainty results for λE are given in Table 1 revealing a standard deviation on the estimate of λE from the ensemble of 60 W m^{-2} and significant sensitivity to the range of inputs used to calculate both β and Φ.

4 Discussion

The results in Fig. 2a may be interpreted through considering the effect of noise in the satellite sounding observations on the estimation of β and hence Λ. From Table 1 we see the ensemble distribution of Λ has a significant negative skew due to taking the inverse of the noise on p_1 and p_2 (c.f. Eq. 6). As a result, there will be a tendency to over specify Λ from the sounding data given the "true" value will be less than the mode. Both the likelihood and the magnitude of this over specification will increase as $p_1 - p_2 \rightarrow 0$ (i.e. as $\Lambda \rightarrow 0$) because of a decreasing signal to noise ratio. This explains why Λ (satellite) and Λ (tower) diverge as $\Lambda \rightarrow 0$. An additional reason for this diver-

BGD
11, 8085–8113, 2014

gence is provided by the fact that H (satellite) < H (tower) due to the effects of warm air entrainment (see later).

The retrieval of λE depends heavily on Φ, hence the increase in the satellite to tower correlation seen for λE relative to Λ. Indeed, Λ is a relatively stable characteristic within site so that the variance of λE is dominated by seasonal and diurnal variations in R_N and Φ (da Rocha et al., 2004; Kumagai et al., 2005). For a detailed discussion of the efficacy of the satellite derived values of Φ we have used here, the reader is referred to Mallick et al. (2014). To summarise, in comparing the satellite derived Φ with the tower $H + \lambda E$, Mallick et al. (2014) found that their satellite estimate underestimated the tower value by, on average, approximately 10 % , i.e. Φ (satellite) $\approx 0.90\Phi$ (tower) (see Fig. 2b). Therefore, the 2 % underestimate in λE (satellite) seen here would indicate that we are getting an approximately 8 % compensation error in λE, introduced by the overspecification of Λ (satellite) seen in Fig. 2a.

Given there appears to be a widespread lack of energy balance closure of the order of 20 % observed at most FLUXNET sites (Wilson et al., 2002), this implies a potential systematic under specification of λE (tower) (and/or H (tower)). However, by the same argument the evaluation between satellite and tower for Φ would change by a similar amount leading to little or no net change in the overall evaluation for λE. Mallick et al. (2014) found that accommodating a 20 % imbalance in Φ (tower) gave Φ (satellite) $\approx 0.72\Phi$ (tower) and that this lack of agreement could be explained by the under specification of the downwelling shortwave radiation component of Φ (satellite). It is unlikely that the entire energy imbalance is attributable solely to λE (tower) (Foken, 2008). As a result, the likely range for the pooled gain between the satellite and tower λE is between 0.8 to 1.0, determined by the combination of under specification of the satellite downwelling shortwave combined with overspecification of satellite Λ.

The monthly infrared products of AIRS are, by definition, a sample of relatively cloud free conditions whilst the tower fluxes are for a mixture of clear and cloudy atmospheric conditions. The inclusion/omission of cloudy conditions should have little or no impact on energy partitioning ratios such as β (Grimmond and Oke, 1995; Balogun et al.,

BGD
11, 8085–8113, 2014

2009). Furthermore, despite being biased low, the shortwave component of Φ specified by Mallick et al. (2014) was for all-sky conditions whilst the IR components of Φ appeared to be somewhat insensitive to the clear sky sampling bias. As a result, the primary motivation for attempting to recover satellite estimates for all-sky conditions would appear to be for increasing the temporal resolution of the data, and not for removing bias from the monthly satellite estimates.

The landscape scale β (and hence Λ) estimated from sounder data relate to a location some few hundred meters above the surface, whilst the tower data relate to heights either meters (for GRA, CRO and SAV) to tens of meters (for EBF, MF, DF, EF) above the surface. These towers are designed to operate in the constant flux portion of the planetary boundary layer which, as a rule-of-thumb, occupies the lower 10 % of the planetary boundary layer and where fluxes change by less than 10 % with height (Stull, 1988). Above this layer there is a tendency of H to decrease with height due to the entrainment of warm air from aloft down into the mixed layer (Stull, 1988). This could partly explain the results in Fig. 2d where H (satellite) is significantly less than H (tower). In contrast, λE often tends to be preserved with height by the entrainment dry air from aloft (Stull, 1988; Mahrt et al., 2001). While comparing ground eddy covariance fluxes with aircraft fluxes over diverse European regions, Gioli et al. (2004) found the value of H at an average height of 70 m was 35 % less that those at ground level, whereas no such trend in λE was observed. Similarly, Migletta et al. (2009) found H lapsed by 36 % as one moved from the surface to a height of 100 m. The same behaviour has also been frequently observed in both airborne and ground-based eddy covariance measurements in USA (e.g. Desjardins et al., 1992) and Europe (Torralba et al., 2008; Migletta et al., 2009). Because of the differing lapse properties of λE and H one would imagine Λ (satellite) should, on average, be more than Λ (tower) which, despite being somewhat uncertain, is what we observe in Fig. 2a.

The Bowen ratio method has been seen to break down under hot, dry conditions. This is due to large scale regionally advected sensible heat desaturating the surface and causing the vertical vapour pressure gradient to reverse (Perez et al., 1999); a con-

BGD
11, 8085–8113, 2014

dition that appeared to persist in the AIRS soundings over central Australia throughout the summer of 2003. Under these conditions k_H can become two to three times higher than k_E so that $k_E \neq k_H$ (Verma et al., 1978). Although we rejected all samples characterised by a reversal of the AIRS vapour pressure gradient, a tendency for Λ (satellite) < Λ (tower) should be observed in the data particularly for the drier biomes. However, for the SAV data Λ (satellite) > Λ (tower) on average (see Fig. 2a) indicating this is not a dominant effect.

The satellite derived fluxes aggregate sub grid heterogeneity (surface geometry, roughness, vegetation index, land surface temperature, surface wetness, albedo etc.) at the 10 000 km^2, whereas the towers aggregate at scales less than 10 km^2. This three orders of magnitude scale mismatch is an important potential source of disagreement between the satellite and tower observed fluxes. Although towers are often installed in relatively homogenous terrain at the local scale, rarely can this be assumed for scales approaching the AIRS data. In addition, characteristics such as surface wetness and temperature can still be highly heterogeneous at the local tower scale (Kustas and Norman, 1999; McCabe and Wood, 2006; Li et al., 2008) whilst also exerting significant nonlinear effects on λE (Nykanen and Georgiou, 2001). If, for example, the probability of a tower being located in either a cool/wet or hot/dry patch is even, and yet the cool/wet regions contribute disproportionately to the satellite scale latent heat flux then, on average, there clearly is a tendency for the tower observed flux to be less than its satellite counterpart (Bastiaanssen et al., 1997). Because of the diversity of nonlinear surface characteristics effects on λE a detailed evaluation lies beyond the scope of this paper. One general inference can be drawn however; the degree of agreement we see in the pooled evaluation would suggest that the spatial scaling from tower to satellite appears somewhat conserved, a feature that is no doubt greatly aided by investigating the monthly average data where the effects of dynamic spatial heterogeneity (e.g. in surface wetness and surface temperature) will tend to have been averaged out. Although a more detailed footprint analysis is required to confirm this, the results in Table 2 suggest that the data from the taller, more extensive forest towers are more closely related

BGD
11, 8085–8113, 2014

to their satellite counterparts, although the higher correlations may simply reflect the dominance of net radiation in driving latent heat flux over these sites.

The pooled RMSD of 79 W m^{-2} for the λE evaluation is comparable with the results reported elsewhere. Mecikalski et al. (1999) reported RMS errors in daily λE estimates in the range of 37 to 59 W m^{-2} while estimating continental scale fluxes over the USA using GOES (Geostationary Operational Environmental Satellite) data. Anderson et al. (2008) reported an RMSD for instantaneous λE estimates of 79 W m^{-2} using a Bowen Ratio closure method and 66 W m^{-2} using the residual surface energy balance method. Another study of Anderson et al. (2007) reported an RMSD in hourly λE of 58 W m^{-2} using 10 km^2 scale GOES data over Iowa, although this reduced to 1.7 W m^{-2} when considering cumulative daily data. Jiang et al. (2009) reported an RMSD of 23–40 W m^{-2} for daily λE retrievals using NOAA (National Oceanic and Atmospheic Administration) AVHRR (Advance Very High Resolution Radiometer) data over southern Florida. Interestingly, they also found a significant negative correlation between satellite and ground-truth evaporative fraction. Jiang and Islam (2001) and Batra et al. (2006) reported RMSD's for noontime λE retrievals from a series of studies over the Southern Great Plains of the USA in the range of 25 to 97 W m^{-2} using moderate resolution NOAA-16, NOAA-14 and MODIS-Terra optical and thermal data. In addressing the effects of scaling and surface heterogeneity issues on λE, McCabe and Wood (2006) obtained an RMSD of 64 W m^{-2} when comparing spatially aggregated LANDSAT (Land Remote-Sensing Satellite) derived instantaneous λE and MODIS Terra λE in central Iowa. Finally, using the surface temperature verses vegetation index triangle approach with MSG (Meteosat Second Generation) SEVIRI (Spinning Enhanced Visible and Infrared Imager) data, Stisen et al. (2008) obtained an RMSD of 41 W m^{-2} for daily data over the Senegal River basin. Finally, Prueger et al. (2005) obtained a disagreement of 45 W m^{-2} in instantaneous noontime λE while comparing 40 m aircraft and 2 m ground eddy covariance λE measurements again in central Iowa.

BGD
11, 8085–8113, 2014

5 Conclusions

We conclude that the combination of the satellite sounding data and the Bowen ratio methodology shows significant promise for retrieving spatial fields of λE when compared with tower ground truth data, and warrants further investigation and refinement. The specification of satellite net available energy, and its shortwave component in particular, requires further attention. There are also circumstances where the satellite Bowen ratio method is inapplicable, but these conditions could be easily flagged by internal checks on the sounding profiles. Where the method appears to work, this provides estimates of λE that would prove valuable in a range of applications. In particular, because no land surface model has been involved in their derivation, the estimates of λE we show can be used as independent data for evaluating land surface parameterisations in a broad range of spatially explicit hydrology, weather and climate models. Furthermore, the availability of sounding data at both 1° and 5 km resolution in conjunction with tower and scintillometer surface flux data would provide an excellent opportunity to explore robust scaling methods in these same models.

Throughout this paper little or no mention is made of the sea latent heat estimates we make because of the lack of appropriate evaluation data sets on which to test these. The SEAFLUX project initiated by the World Climate Research Programme (WCRP) Global Energy and Water Experiment (GEWEX) Radiation Panel is addressing this in the near future. If our sea estimates pass such an evaluation then, again, we would imagine they would be similarly useful in weather and climate model development. Given the Bowen ratio method should work best in these moist environments we predict the sea estimates of latent heat we show here are potentially more reliable than their terrestrial counterparts.

The advent of microwave sounding platforms such as Megha Tropiques may afford an opportunity to extend the methodology to persistent overcast conditions, allowing for more detailed process studies. This approach could also exploit high spatial and temporal resolution geostationary sounder platforms like GOES and, in the near future,

BGD
11, 8085–8113, 2014

GIFTS (Geosynchronous Interferometric Fourier Transform Spectrometer) and INSAT (Indian National Satellite)-3D. We also expect that the high vertical resolution soundings these platforms will provide will improve the accuracy of the current approach, particularly over elevated terrain.

Acknowledgements. We would also like to acknowledge Goddard Earth Sciences – Data & Information Services Centre (GESS – DISC), Level 1 and Atmosphere Archive and Distribution System (LAADS) web interface, NASA, and for putting the AIRS and MODIS data into the public domain. We kindly acknowledge all the site PI's who have provided terrestrial flux data through the FLUXNET data archive. The AmeriFlux regional network component of this archive is supported with funding from the US Department of Energy under its Terrestrial Carbon project.

References

Anderson, M. C., Norman, J. M., Mecikalski, J. R., Otkin, J. P., and Kustas, W. P.: A climatological study of evapotranspiration and moisture stress across the continental US based on thermal remote sensing: I. Model formulation, J. Geophys. Res., 112, D11112, doi:10.1029/2006JD007506, 2007.

Anderson, M. C., Norman, J. M., Kustas, W. P., Houborg, R., Starks, P. J., and Agam, N.: A thermal-based remote sensing technique for routine mapping of land-surface carbon, water and energy fluxes from field to regional scales, Remote Sens. Environ., 112, 4227–4241, 2008.

Aumann, H. H., Chahine, M. T., Gautier, C., Goldberg, M. D., Kalnay, E., McMillin, L. M., Revercomb, H., Rosenkranz, P. W., Smith, W. L., Staelin, D. H., Strow, L., L., and Susskind, J.: AIRS/AMSU/HSB on the aqua mission: design, science objectives, data products and processing systems, IEEE T. Geosci. Remote, 41, 253–264, 2003.

Baldocchi, D. D., Falge, E., Gu, L., Olson, R., Hollinger, D., Running, S., Anthoni, P., Bernhofer, C., Davis, K., Evans, R., Fuentes, J., Goldstein, A., Katul, G., Law, B., Lee, X., Malhi, Y., Meyers, T., Munger, W., Oechel, W., Paw, U. K. T., Pilegaard, K., Schmid, H. P., Valentini, R., Verma, S., Vesala, T., Wilson, K., and Wofsy, S.: Fluxnet: a new tool to study the temporal and spatial variability of ecosystem-scale carbon dioxide, water vapor, and energy flux densities, B. Am. Meteorol. Soc., 82, 2415–3434, 2001.

BGD
11, 8085–8113, 2014

Balogun, A. A., Adegoke, J. O., Vezhapparambu, S., Mauder, M., McFadden, J. P., and Gallo, K.: Surface energy balance measurements above an exurban residential neighbourhood of Kansas City, Missouri, Bound.-Lay. Meteorol., 133, 299–321, 2009.
Bastiaanssen, W. G. M., Pelgrum, H., Droogers, P., de Bruin, H. A. R., and Menenti, M.: Area-average estimates of evaporation, wetness indicators and top soil moisture during two golden days in EFEDA, Agr. Forest Meteorol., 87, 119–137, 1997.
Bastiaanssen, W. G. M., Menenti, M., Feddes, R. A., and Holtslag, A. A. M.: The Surface Energy Balance Algorithm for Land (SEBAL): Part 1 formulation, J. Hydrol., 212–213, 198–212, 1998.
Batra, N., Islam, S., Venturini, V., Bisht, G., and Jiang, L.: Estimation and comparison of evapotranspiration from MODIS and AVHRR sensors for clear sky days over the southern great plains, Remote Sens. Environ., 103, 1–15, 2006.
Betts, A. K. and Ridgway, W.: Climate equilibrium of the atmospheric convective boundary layer over a tropical ocean, J. Atmos. Sci., 46, 2621–2641, 1999.
Bowen, I. S.: The ratio of heat losses by conduction and by evaporation from any water surface, Phys. Rev., 27, 779–787, 1926.
Brennan, M. J. and Lackmann, G. M.: The influence of incipient latent heat release on the precipitation distribution of the 24–25 January 2000 US East Coast cyclone, Mon. Weather Rev., 133, 1913–1937, 2005.
Campbell Scientific: Bowen Ratio Instrumentation Instruction Manual, Campbell Scientific Inc., 815 West 1800 North, Logan, Utah, 84321-1784.
Chen, F. and Dudhia, J.: Coupling an advanced land surface–hydrology model with the Penn State–NCAR MM5 modeling system. part I: model implementation and sensitivity, Mon. Weather Rev., 129, 569–585, 2001.
Choudhury, B. J. and DiGirolamo, N.: A biophysical process-based estimate of global land surface evaporation using satellite and ancillary data I. Model description and comparison with observations, J. Hydrol., 205, 164–185, 1998.
da Rocha, H. R., Goulden, M. L., Miller, S. D., Menton, M. C., Pinto, L. D. V. O., De Freitas, H. C., and Silva Figueira, A. M. E.: Seasonality of water and heat fluxes over a tropical forest in eastern Amazonia, Ecol. Appl., 14, 22–32, 2004.
da Rocha, H. R., Manzi, A. O., Cabral, O. M., Miller, S. D., Goulden, M. L., Saleska, S. R., Coupe, N. R., Wofsy, S. C., Borma, L. S., Artaxo, P., Vourlitis, G., Nogueira, J. S., Cardoso, F. L., Nobre, A. D., Kruijt, B., Freitas, H. C., von Randow, C., Aguiar, R. G., and

BGD
11, 8085–8113, 2014

Maia, J. F.: Patterns of water and heat flux across a biome gradient from tropical forest to savanna in Brazil, J. Geophys. Res.-Atmos., 114, G00B12, doi:10.1029/2007JG000640, 2009.
Desjardins, R. L., Hart, R. L., Macpherson, J. I., Schuepp, P. H., and Verma, S. B.: Aircraft-based and tower-based fluxes of carbondioxide, latent, and sensible heat, J. Geophys. Res.-Atmos., 97, 18477–18485, 1992.
Dyer, A. J.: A Review of flux profile relationships, Bound.-Lay. Meteorol., 7, 363–372, 1974.
Feng, M., Biastoch, A., Böning, C., Caputi, N., and Meyers, G.: Seasonal and interannual variations of upper ocean heat balance off the west coast of Australia, J. Geophys. Res., 113, C12025, doi:10.1029/2008JC004908, 2008.
Fink, A. H., Brücher, T., Krüger, A., Leckebusch, G. C., Pinto, J. G., and Ulbrich, U.: The 2003 European summer heatwaves and drought – synoptic diagnosis and impacts, Weather, 59, 209–216, 2004.
Fisch, G., Tota, J., Machado, L. A. T., Silva Dias, M. A. F., da F Lyra, R. F., Nobre, C. A., Dolman, A. J., and Gash, J. H. C.: The convective boundary layer over pasture and forest in Amazonia, Theor. Appl. Climatol., 78, 47–59, 2004.
Foken, T.: The energy balance closure problem: an overview, Ecol. Appl., 18, 1351–1367, 2008.
Foken, T., Wimmer, F., Mauder, M., Thomas, C., and Liebethal, C.: Some aspects of the energy balance closure problem, Atmos. Chem. Phys., 6, 4395–4402, doi:10.5194/acp-6-4395-2006, 2006.
Fritschen, L. J. and Fritschen, C. L.: Bowen ration energy balance method, in: Micrometeorology in Agricultural Systems, edited by: Hatfield, J. L. and Baker, J. M., American Soc. Agronomy, Madison, Wisconsin, USA, 397–406, 2005.
Giambelluca, T. W., Scholz, F. G., Bucci, S., Meinzer, F. C., Goldstein, G., Hoffmann, W. A., Franco, A. C., and Buchert, M. P.: Evapotranspiration and energy balance of Brazilian savannas with contrasting tree density, Agr. Forest Meteorol., 149, 1365–1376, 2009.
Gioli, B., Miglietta, F., Martino, B. D., Hutjes, R. W. A., Dolman, H. A. J., Lindroth, A., Schumacher, M., Sanz, M. J., Manca, G., Peressotti, A., and Dumas, E. J.: Comparison between tower and aircraft-based eddy covariance fluxes in five European regions, Agr. Forest Meteorol., 127, 1–16, 2004.
Grimmond, C. S. B. and Oke, T. R.: Comparison of heat fluxes from summertime observations in the suburbs of four north American cities, J. Appl. Meteorol., 34, 873–889, 1995.

BGD
11, 8085–8113, 2014

Hoen, J. O. Y., Hai, Y. X., Pan, J., Xia, H. M., and Liu, T. W.: Calculation of the Bowen ratio in the tropical Pacific using sea surface temperature data, J. Geophys. Res., 107, 17.1–17.16, 2002.

Hsu, S. A.: A relationship between the Bowen ratio and sea–air temperature difference under unstable conditions at sea, J. Phys. Oceanogr., 28, 2222–2226, 1998.

Irannejad, P., Henderson-Sellers, A., and Sharmeen, S.: Importance of land-surface parameterization for latent heat simulation in global atmospheric models, Geophys. Res. Lett., 30, 1904, doi:10.1029/2003GL018044, 2003.

Jiang, L. and Islam, S.: Estimation of surface evaporation map over southern Great Plains using remote sensing data, Water Resour. Res., 37, 329–340, 2001.

Jiang, L., Islam, S., Guo, W., Jutla, A. S., Senarath, S. U. S., Ramsay, B. H., and Eltahir, E.: A satellite-based daily actual evapotranspiration estimation algorithm over South Florida, Global Planet. Change, 67, 62–77, 2009.

Jiminez, C., Prigent, C., and Aries, F.: Towards an estimation of global land surface heat fluxes from multisatellite observations, J. Geophys. Res., 114, D06305, doi:10.1029/2008JD011392, 2009.

Kohler, M., Kalthoff, N., and Kottmeier, C.: The impact of soil moisture modifications on CBL characteristics in West Africa: a case-study from the AMMA campaign, Q. J. Roy. Meteor. Soc., 136, 442–455, 2009.

Konda, M.: The satellite-derived air temperature and the Bowen ratio over the ocean, in: 35th COSPAR Scientific Assembly, 18–25 July 2004, Paris, France, 1839, 2004.

Kumagai, T., Saitoh, T. M., Sato, Y., Takahashi, H., Manfroi, O. J., Morooka, T., Kuraji, K., Suzuki, M., Yasunari, T., and Komatsu, H.: Annual water balance and seasonality of evapotranspiration in a Bornean tropical rainforest, Agr. Forest Meteorol., 128, 81–92, 2005.

Kustas, W. P. and Norman, J. M.: Evaluating the effects of subpixel heterogeneity on pixel average fluxes, Remote Sens. Environ., 74, 327–342, 1999.

Lawford, R. G., Stewart, R., Roads, J., Isemer, H.-J., Manton, M., Marengo, J., Yasunari, T., Benedict, S., Koike, T., and Williams, S.: Advancing global and continental scale hydrometeorology: contributions of the GEWEX Hydrometeorology Panel, B. Am. Meteorol. Soc., 85, 1917–1930, 2004.

Lehner, B., Döll, P., Alcamo, J., Henrichs, T., and Kaspar, F.: Estimating the impact of global change on flood and drought risks in Europe: a continental, integrated analysis, Climatic Change, 75, 273–299, 2005.

BGD
11, 8085–8113, 2014

Li, F., Kustas, W. P., Anderson, M. C., Prueger, J. H., and Scott, R. L.: Effect of remote sensing spatial resolution on interpreting tower-based flux observations, Remote Sens. Environ., 112, 337–349, 2008.

Mahrt, L., Vickers, D., and Sun, J.: Spatial variations of surface moisture flux from aircraft data, Adv. Water Resour., 24, 1133–1141, 2001.

Mallick, K., Bhattacharya, B. K., Chaurasia, S., Dutta, S., Nigam, R., Mukherjee, J., Banerjee, S., Kar, G., Rao, V. U. M., Gadgil, A. S., and Parihar, J. S.: Evapotranspiration using MODIS data and limited ground observations over selected agroecosystems in India, Int. J. Remote Sens., 28, 2091–2110, 2007.

Mallick, K., Bhattacharya, B. K., Rao, V. U. M., Reddy, D. R., Banerjee, S., Hoshali, V., Pandey, V., Kar, G., Mukherjee, J., Vyas, S. P., Gadgil, A. S., and Patel, N. K.: Latent heat flux estimation in clear sky days over Indian agroecosystems using noontime satellite remote sensing data, Agr. Forest Meteorol., 149, 1646–1665, 2009.

Mallick, K., Jarvis, A. J., Wohlfahrt, G., Gough, C., Hirano, T., Kiely, G., Miyata, A., Yamamoto, S., and Hoffmann, L.: Components of near-surface energy balance derived from satellite soundings: i. Net available energy, Biogeosciences, submitted, 2014.

McCabe, M. F. and Wood, E. F.: Scale influences on the remote estimation of evapotranspiration using multiple satellite sensors, Remote Sens. Environ., 105, 271–285, 2006.

McCabe, M. F., Wood, E. F., Wójcik, R., Pan, M., Sheffield, J., Gao, H., and Su, H.: Hydrological consistency using multi-sensor remote sensing data for water and energy cycle studies, Remote Sens. Environ., 112, 430–444, 2008.

Mecikalksi, J. R., Diak, G. R., Anderson, M. C., and Norman, J. M.: Estimating fluxes on continental scales using remotely-sensed data in an atmospheric–land exchange model, J. Appl. Meteorol., 35, 1352–1369, 1999.

Miglietta, F., Gioli, B., Brunet, Y., Hutjes, R. W. A., Matese, A., Sarrat, C., and Zaldei, A.: Sensible and latent heat flux from radiometric surface temperatures at the regional scale: methodology and evaluation, Biogeosciences, 6, 1975–1986, doi:10.5194/bg-6-1975-2009, 2009.

Mu, Q., Heinsch, F. A., Zhao, M., and Running, S. W.: Development of a global evapotranspiration algorithm based on MODIS and global meteorology data, Remote Sens. Environ., 111, 519–536, 2007.

Nickel, D., Barthel, R., and Braun, J.: Large-scale water resources management within the framework of GLOWA-Danube – the water supply model, Phys. Chem. Earth, 30, 383–388, 2005.

BGD
11, 8085–8113, 2014

Nykanen, D. K. and Georgiou, E. F.: Soil moisture variability and scale-dependency of nonlinear parameterizations in coupled land–atmosphere models, Adv. Water. Res., 24, 1143–1157, 2001.
Perez, P. J., Castellvi, F., Ibanez, M., and Rosell, J. I.: Assessment of reliability of Bowen ratio method for partitioning fluxes, Agr. Forest Meteorol., 97, 141–150, 1999.
Prueger, J. H., Hatfield, J. L., Kustas, W. P., Hipps, L. E., Macpherson, J. I., Neale, C. M. U., Eichinger, W. E., Cooper, D. I., and Parkin, T. B.: Tower and aircraft eddy covariance measurements of water vapor, energy, and carbon dioxide fluxes during SMACEX, J. Hydrometeorol., 6, 954–960, 2005.
Rider, N. E. and Philip, J. R.: Advection and evaporation, Assn. Internat. Hydrologie Sci., 53, 421–427, 1960.
Russel, J. M. and Johnson, T. C.: The water balance and stable isotope hydrology of Lake Edward, Uganda-Congo, J. Great Lakes Res., 32, 77–90, 2006.
Salby, M. L.: Fundamental of Atmospheric Physics, Academic Press, 1996.
Shuttleworth, W. J., Gurney, R. J., Hsu, A. Y., and Ormsby, J. P.: FIFE: the variation in energy partition at surface flux sites, in: Remote Sensing and Large-Scale Processes, edited by: Rango, A., Proceedings of the IAHS third International Assembly, Baltimore, MD, May, IAHS Publication, 186, 67–74, 1989.
Stisen, S., Sandholt, I., Nørgaard, A., Fensholt, R., and Jensen, K. H.: Combining the triangle method with thermal inertia to estimate regional evapotranspiration applied to MSG-SEVIRI data in the Senegal River Basin, Remote Sens. Environ., 112, 1242–1255, 2008.
Stull, R. B.: An Introduction to Boundary Layer Meteorology, Kluwer Academic Publishers, Dordrecht, 1988.
Swinbank, W. C. and Dyer, A. J.: An experimental study in micrometeorology, Q. J. Roy. Meteor. Soc., 93, 494–500, 1967.
Tanner, C. B.: A simple aero-heat budget method for determining daily evapotranspiration, Trans. Int. Congr. Soil Sci., 1, 203–209, 1961.
Tasumi, M., Allen, R. G., Trezza, R., and Wright, J. L.: Satellite-based energy balance to assess within-population variance of crop coefficient curves, J. Irrig. Drain. E.-ASCE, 131, 94–109, 2005.
Tobin, D. C., Revercomb, H. E., Knuteson, R. O., Lesht, B. M., Strow, L. L., Hannon, S. E., Feltz, W. F., Moy, L. A., Fetzer, E. J., and Cress, T. S.: Atmospheric radiation measurement site atmospheric state best estimates for atmospheric infrared sounder temperature and wa-

BGD
11, 8085–8113, 2014

ter vapor retrieval validation, J. Geophys. Res., 111, D09S14, doi:10.1029/2005JD006103, 2006.
Todd, R., Evett, S. R., and Howell, T. A.: The Bowen ratio-energy balance method for estimating latent heat flux of irrigated alfalfa evaluated in a semi-arid, advective environment, Agr. Forest Meteorol., 103, 335–348, 2000.
Torralba, P. C., de Arellano, J. V. G., Bosveld, F., Soler, M. R., Vermeulen, A., Werner, C., and Moors, E.: Diurnal and vertical variability of the sensible heat and carbon dioxide budgets in the atmospheric surface layer, J. Geophys. Res., 113, D12119, doi:10.1029/2007JD009583, 2008.
Verma, S. B., Rosenberg, N. J., and Blad, B. L.: Turbulent exchange coefficients for sensible heat and water vapor under advective conditions, J. Appl. Meteorol., 17, 330–338, 1978.
Verstraeten, W. W., Veroustraete, F., and Feyen, J.: Estimating evapotranspiration of European forests from NOAA-imagery at satellite overpass time: towards an operational processing chain for integrated optical and thermal sensor data products, Remote Sens. Environ., 96, 256–276, 2005.
Wilson, K. B., Goldstein, A. H., Falge, E., Aubinet, M., Baldocchi, D., Berbigier, P., Bernhofer, Ch., Ceulemans, R., Dolman, H., Field, C., Grelle, A., Law, B., Meyers, T., Moncrieff, J., Monson, R., Oechel, W., Tenhunen, J., Valentini, R., and Verma, S.: Energy balance closure at FLUXNET sites, Agr. Forest Meteorol., 113, 223–243, 2002.
Wohlfahrt, G., Haslwanter, A., Hörtnagl, L., Jasoni, R. L., Fenstermaker, L. F., Arnone III, J. A., and Hammerle, A.: On the consequences of the energy imbalance for calculating surface conductance to water vapour, Agr. Forest Meteorol., 149, 1556–1559, 2009.

BGD
11, 8085–8113, 2014

Table 1. Sensitivity analysis results of Λ, Φ and λE. The forcing data are taken for mid-summer, Southern Great Plains, US. Sensitivities are locally linear averaged across the ensemble response and expressed as dimensionless relative changes. Only absolute sensitivities > 0.1 are shown. $N = 10^5$ realisations.

		Λ	Φ (W m^{-2})	λE (W m^{-2})
x	sample range	$\mathrm{d}\Lambda/\mathrm{d}x$	$\mathrm{d}\Phi/\mathrm{d}x$	$\mathrm{d}\lambda E/\mathrm{d}x$
τ_A	±10 %	–	1.58	1.56
f	±10 %	–	−0.94	−0.92
α	±10 %	–	−0.31	−0.29
ε_S	±10 %	–	−0.37	−0.34
ε_A	±10 %	–	1.19	1.20
T_S	±1 K	–	−0.21	−0.19
T_{925}	±1 K	0.45	–	0.54
T_{1000}	±1 K	−0.46	–	−0.45
p_{925}	±10 %	1.23	–	1.22
p_{1000}	±10 %	−1.04	–	−1.02
		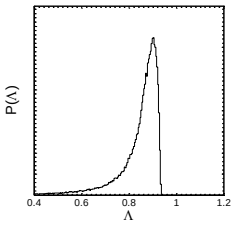	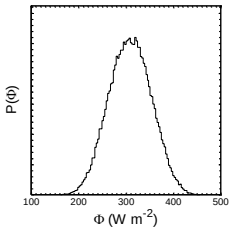	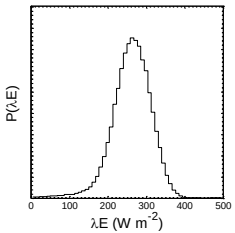
standard deviation		0.11	44 W m^{-2}	60 W m^{-2}

BGD
11, 8085–8113, 2014

Table 2. Error analysis of AIRS derived λE and H over diverse plant functional types (biomes) of FLUXNET eddy covariance network. Values in the parenthesis are ±one standard deviation unless otherwise stated.

	λE				H			
Biome	RMSD ($W\,m^{-2}$)	Slope	r	N	RMSD ($W\,m^{-2}$)	Slope	r	N
EBF	84.84	1.02 (±0.04)	0.70 (±0.09)	65	53.2	0.64 (±0.03)	0.73 (±0.09)	66
MF	60.66	0.92 (±0.09)	0.65 (±0.14)	32	87.9	0.50 (±0.04)	0.67 (±0.14)	30
GRA	78.39	0.87 (±0.08)	0.67 (±0.12)	42	55.82	0.79 (±0.09)	0.43 (±0.15)	39
CRO	69.76	0.85 (±0.08)	0.59 (±0.15)	31	51.74	0.93 (±0.06)	0.79 (±0.11)	31
ENF	67.64	1.02 (±0.07)	0.76 (±0.10)	43	95.14	0.52 (±0.04)	0.62 (±0.13)	37
DBF	65.19	0.86 (±0.06)	0.68 (±0.09)	74	73.19	0.59 (±0.04)	0.49 (±0.11)	70
SAV	140.78	2.00 (±0.28)	0.41 (±0.22)	19	148.52	0.45 (±0.05)	0.51 (±0.22)	18
Pooled	78.74	0.98 (±0.02)	0.75 (±0.04)	306	76.94	0.59 (±0.02)	0.56 (±0.05)	291

EBF = Evergreen broadleaf forest, MF = Mixed forest, GRA = Grassland, CRO = Cropland, ENF = Evergreen needleleaf forest, DBF = Deciduous broadleaf forest, SAV = Savanna.

BGD
11, 8085–8113, 2014

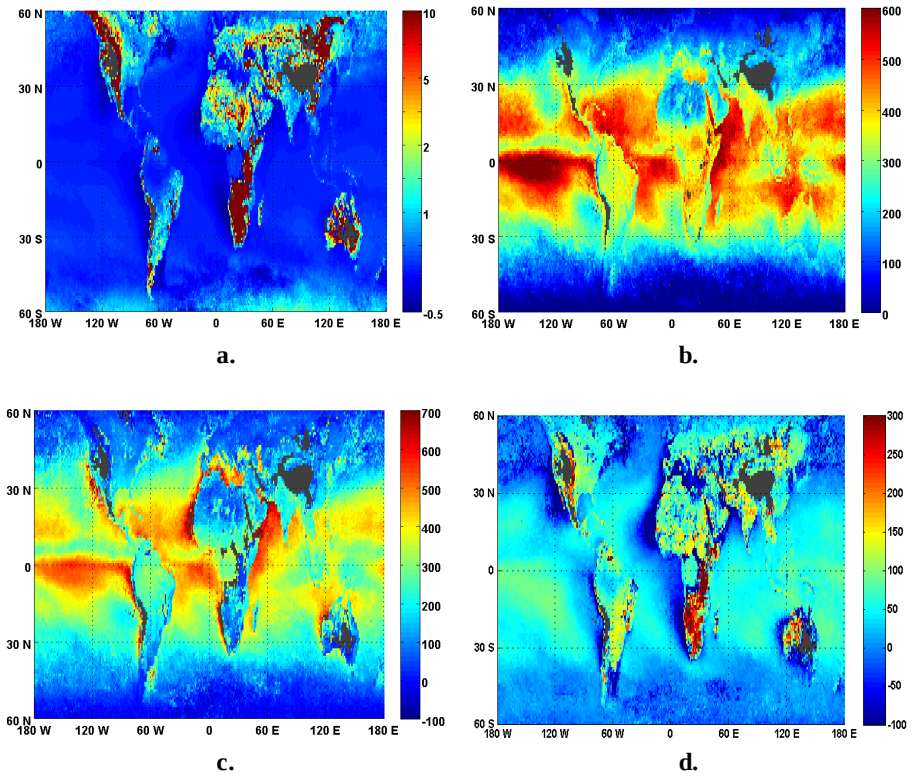

Figure 1. Global fields of yearly average 13:30 LT derived from AIRS sounder observations for 2003. **(a)** Bowen ratio β ($W\,m^{-2}\,W^{-1}\,m^2$). **(b)** Net available energy, Φ ($W\,m^{-2}$). **(c)** Latent heat flux, λE ($W\,m^{-2}$). **(d)** Sensible heat flux, H ($W\,m^{-2}$). Missing data are marked in grey.

BGD
11, 8085–8113, 2014

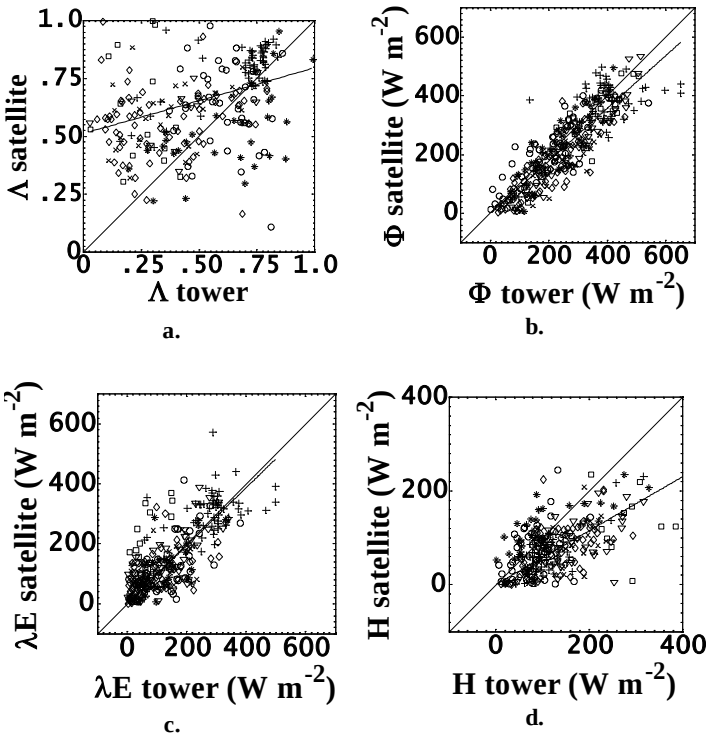

Figure 2. The evaluation of the AIRS derived monthly 13:30 LT components against their tower equivalent. **(a)** Evaporative fraction, Λ. Here, the solid line denotes Λ (satellite) = 0.31(±0.02)Λ (tower) + 0.49(±0.04). **(b)** Net available energy, Φ. Here, the solid line denotes Φ (satellite) = 0.90(±0.03)Φ (tower) − 2.43(±8.19) (see Mallick et al., 2014). **(c)** Latent heat flux, λE. **(d)** Sensible heat flux, H. For regression statistics see Table 2. 1 : 1 line shown for reference.

(+ EBF; × MF; ○ GRA; ∗ CRO; ∇ ENF; ◊ DBF; □ SAV)

BGD
11, 8085–8113, 2014

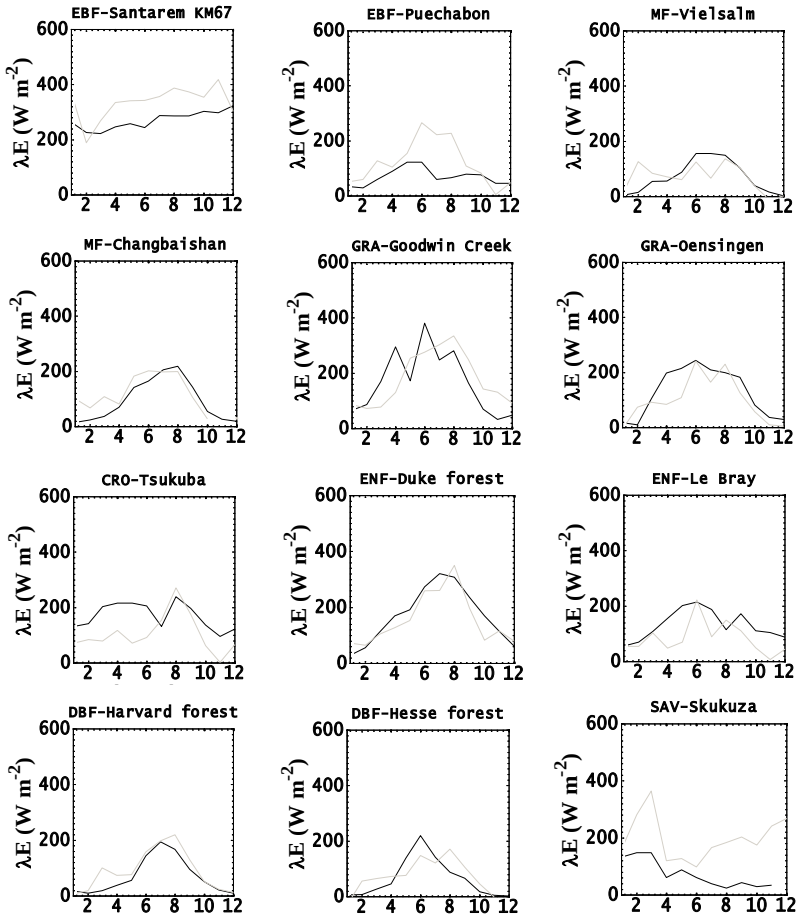

Figure 3. Satellite (grey) and tower (black) time series of monthly average 13:30 LT latent heat flux, λE, for a selection of sites for 2003. The numbers in the x-axis are the month numbers.

BGD
11, 8085–8113, 2014